

## Luminescence Processes in the Crystalline and Glass Modifications of $LnBGeO_5$ -Type Compositions

J. W. M. VERWEY,<sup>1</sup> D. VAN DER VOORT, G. J. DIRKSEN,  
AND G. BLASSE

*Debye Research Institute, University of Utrecht, P.O. Box 80.000,  
3508 TA Utrecht, The Netherlands*

Received May 24, 1990

The luminescence properties of the  $Eu^{3+}$  ion in the crystalline and glass modifications of  $LnBGeO_5$ -type compositions ( $Ln = La, Gd, Y$ , and  $CaBPO_5$ ) are investigated. The efficiency of the luminescence upon broad band excitation is higher in the crystals than it is in the glasses. Whereas crystalline  $GdBGeO_5:Eu$  is a very efficient luminescent material, crystalline  $LaBGeO_5:Eu$  and  $CaBPO_5:Eu$  show only medium efficiency, and the glass modifications are of a low to very low efficiency. The influence of the charge and the size of the ion for which  $Eu^{3+}$  is substituted is discussed. The influence of these cations on the efficiency of the luminescence of the  $Eu^{3+}$  ion is well known for crystalline compositions, but is observed for the first time in the glass modifications, where they play the role of network modifiers. The undoped compositions show a blue luminescence. Further we observed  $Eu^{2+}$  emission in the europium-doped  $CaBPO_5$  glass. It shows inhomogeneous broadening, so that not only broad band but also a small amount of sharp line emission could be observed. © 1990 Academic Press, Inc.

### 1. Introduction

Recently Rulmont and Tarte (1) and Lysanova *et al.* (2) have reported a study of lanthanide borogermanates  $LnBGeO_5$  by X-ray powder diffraction and vibrational spectroscopy. For the larger lanthanide ions they find the stillwellite structure of  $CeBSiO_5$  (3), but for the smaller ones another, monoclinic phase. For the smallest ions (Tm, Yb, Lu) the compound does not exist. Both modifications of  $LnBGeO_5$  contain  $BO_4$  and  $GeO_4$  tetrahedra in an ordered arrangement. Also the borophosphates  $M(II)BPO_5$  ( $M = Ca, Sr, Ba, Pb$ ) have the stillwellite structure (1).

In this paper we report on the  $Eu^{3+}$  lumi-

nescence of these compositions. Our aim for this study was twofold. Borogermanates may be expected to form glass modifications easily. This opens the way to study the  $Eu^{3+}$  luminescence in the crystalline and the glass modifications of one and the same composition. We have recently shown that this is an approach which yields information on the nonradiative processes in the  $Eu^{3+}$  charge-transfer (CT) state (4, 5). By comparing the  $Eu^{3+}$  luminescence in crystalline  $LnBGeO_5$  and  $MBPO_5$  it is also possible to study how an effective charge on the  $Eu^{3+}$  ion influences the luminescence properties. This type of research was started by us recently (6).

In addition we studied the luminescence of some other activators in the borogermanates which seem to be an interesting type

<sup>1</sup> To whom correspondence should be addressed.

of host lattice for this purpose. The main results of our investigations relate to the nonradiative processes in the CT state of the  $Eu^{3+}$  ion. In crystalline  $GdBGeO_5:Eu$  the CT state feeds the emitting levels, but in the glass modifications mainly the ground state, so that the emission is quenched. In crystalline  $LaBGeO_5:Eu$  and  $CaBPO_5:Eu$  the situation is in between.

## 2. Experimental

The crystalline modifications of  $LnBGeO_5$  were prepared following Ref. (1). The crystalline modification  $CaBPO_5$  doped with  $Eu^{3+}$  or  $Eu^{3+}, Na^+$  was prepared from the following starting materials:  $CaCO_3$  (Merck, Suprapur),  $(NH_4)_2HPO_4$ ,  $H_3BO_3$ ,  $Na_2CO_3$  (all Merck, p.a.), and  $Eu_2O_3$  (Highways International 5N). The compounds  $CaCO_3$  and  $Eu_2O_3$  (and  $Na_2CO_3$ ) were weighed stoichiometrically and dissolved into a small amount of hot hydrochloric acid (Baker Reagents). To this solution a solution of  $H_3BO_3$  and  $(NH_4)_2HPO_4$  in distilled water was added. Under stirring this solution was dried and then fired for 1 hr in air at  $800^\circ C$ . The powder was ground and fired again for 1 hr. The crystal structure was checked with X-ray powder diffraction using  $CuK\alpha$  radiation. Densities of powdered glasses and crystals were determined pycnometrically.

The  $GdBGeO_5$  and  $LaBGeO_5$  glasses (doped and undoped) were prepared by melting the stoichiometric mixture for  $\sim 20$  min at  $1250^\circ C$  in air. The  $YBGeO_5$  and  $CaBPO_5$  glasses were too viscous to pour at temperatures below  $1400^\circ C$ . Because of this high temperature, 5 to 10% excess of  $H_3BO_3$  and  $GeO_2$  or  $H_3BO_3$  and  $(NH_4)HPO_4$  was added to account for evaporation, respectively. These two glasses were cooled between bronze plates, which resulted in homogeneous transparent disks  $\sim 12$  mm in diameter and 3 mm thick. A certain amount of the europium became divalent in the  $CaBPO_5$  glass, even when melted in air.

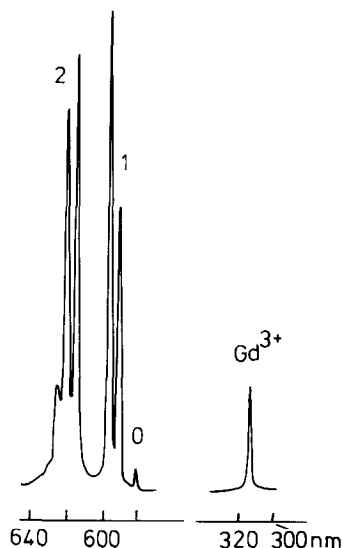


FIG. 1. Emission spectrum of  $Gd_{0.99}Eu_{0.01}BGeO_5$  (crystalline) at 300 K.  $\lambda_{exc} = 275$  nm. Shorter wavelength side  $Gd^{3+}$  emission, longer wavelength side  $Eu^{3+}$  emission (with J in  $^3D_0 \rightarrow ^7F_1$  indicated). Note break in wavelength scale.

The emission and excitation spectra were recorded using a MPF-3L spectrofluorometer, equipped with a helium flow cryostat (Oxford CF 100). For some excitation spectra a setup described before (6) was used, consisting of a tunable dye laser pumped with a pulsed nitrogen laser, a Thor bath cryostat, and a 1-m Spex monochromator. Diffuse reflection spectra were recorded using a Perkin-Elmer Lambda 7 UV/VIS spectrophotometer. Quantum efficiencies were determined by comparison with standard phosphors.

## 3. Results and Discussion

### 3.1. $Gd_{0.99}Eu_{0.01}BGeO_5$ (Crystalline)

In crystalline  $GdBGeO_5$  the  $Eu^{3+}$  ion shows an intense red luminescence for short-wavelength ultraviolet (i.e., CT) excitation. This luminescence was also reported by Lysanova *et al.* (2), but no analysis was given.

Figure 1 shows the emission spectrum at

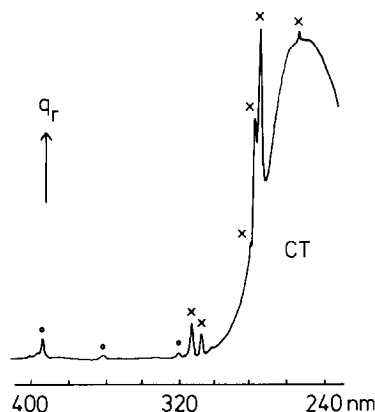


FIG. 2. Excitation spectrum of  $\text{Eu}^{3+}$  in  $\text{Gd}_{0.99}\text{Eu}_{0.01}\text{BGeO}_5$  (crystalline) at 300 K.  $\text{Gd}^{3+}$  lines indicated by crosses,  $\text{Eu}^{3+}$  lines by circles; CT is  $\text{Eu}^{3+}$  charge-transfer band.  $q_r$  denotes the relative quantum output.

300 K for 275-nm excitation. It consists of a weak  $\text{Gd}^{3+}$  emission line at 312.5 nm (see below) and the well-known  ${}^5\text{D}_0$ - ${}^7\text{F}_j$  lines of  $\text{Eu}^{3+}$ . The  $\text{Gd}^{3+}$  emission has disappeared for 250-nm excitation. Higher level emission from  $\text{Eu}^{3+}$  is absent due to the presence of high-frequency vibrational modes in the host lattice (up till  $1120\text{ cm}^{-1}$  (1)), which facilitates nonradiative decay to the  ${}^5\text{D}_0$  level (7).

The  $\text{Eu}^{3+}$  emission pattern shows one  ${}^5\text{D}_0$ - ${}^7\text{F}_0$ , two  ${}^5\text{D}_0$ - ${}^7\text{F}_1$ , and three  ${}^5\text{D}_0$ - ${}^7\text{F}_2$  lines. This suggests  $\text{C}_{3(v)}$  as a site symmetry for  $\text{Eu}^{3+}$  (and  $\text{Gd}^{3+}$ ) in  $\text{GdBGeO}_5$ . The crystal field splitting of the  ${}^7\text{F}_1$  level is about  $155\text{ cm}^{-1}$ .

The excitation spectrum of the  $\text{Eu}^{3+}$  emission at 300 K is given in Fig. 2. Apart from very weak features due to transitions within the  $4f^n$  configuration of  $\text{Eu}^{3+}$ , the excitation spectrum consists of lines due to  $\text{Gd}^{3+}$  and a broad band due to  $\text{Eu}^{3+}$  (CT transition). Its maximum is at about 250 nm. The quantum efficiency for CT excitation amounts to 80% or higher.

This band is not due to host lattice absorption. Diffuse reflection spectra show that the latter absorption starts at 300 K at  $\lambda = 200$

nm. At 4.2 K the excitation spectrum of the  $\text{Eu}^{3+}$  emission changes in one aspect, viz. the intensity of the  $\text{Gd}^{3+}$  excitation lines drops considerably by about one order of magnitude. In the emission spectrum the relative changes are even more apparent. Excitation with 250 nm yields only  $\text{Eu}^{3+}$  emission, but 275 nm yields equal amounts of  $\text{Gd}^{3+}$  and  $\text{Eu}^{3+}$  emission intensities. The excitation spectrum of the  $\text{Gd}^{3+}$  emission consists of the  ${}^8\text{S} \rightarrow {}^6\text{P}$ ,  ${}^6\text{I}$ , and  ${}^6\text{D}$  transitions.

The excitation process can easily be understood following considerations given before (7, 8). Excitation with 250 nm corresponds to  $\text{Eu}^{3+}$  CT excitation. The CT-excited state relaxes nonradiatively to the excited levels of the  $4f^6$  configuration, feeding the emitting  ${}^5\text{D}_0$  level. The absorption strength of  $\text{Gd}^{3+}$   $4f^7$  transitions is negligible compared to that of the CT transition, so that no  $\text{Gd}^{3+}$  emission is observed.

Excitation with 275 nm results mainly in  $\text{Gd}^{3+}$  excitation ( ${}^8\text{S}$ - ${}^6\text{I}$ ), since this wavelength corresponds only to the tail of the  $\text{Eu}^{3+}$  CT transition (at 4.2 K even less than at 300 K). At 4.2 K  $\text{Gd}^{3+}$  excitation yields mainly  $\text{Gd}^{3+}$  emission, but at 300 K energy migration over the sublattice transports the excitation energy to the  $\text{Eu}^{3+}$  ions. At 4.2 K this migration is no longer effective, since shallow  $\text{Gd}^{3+}$  traps hamper the migration process. The  $\text{Gd}^{3+}$  emission originates from these traps (4, 9).

### 3.2. $\text{La}_{0.99}\text{Eu}_{0.01}\text{BGeO}_5$ (Crystalline)

In crystalline  $\text{LaBGeO}_5$  the  $\text{Eu}^{3+}$  ion shows a red emission of medium intensity upon CT excitation. Figure 3 shows the  $\text{Eu}^{3+}$  emission spectrum at 300 K which does not change upon cooling. There are one  ${}^5\text{D}_0$ - ${}^7\text{F}_0$ , three  ${}^5\text{D}_0$ - ${}^7\text{F}_1$ , and three  ${}^5\text{D}_0$ - ${}^7\text{F}_2$  lines. The crystallographic data (3) do not give any symmetry element for the lanthanide site. So we have to expect five  ${}^5\text{D}_0$ - ${}^7\text{F}_2$  lines. Obviously the approximate site symmetry is higher than  $\text{C}_1$ . The splitting of the  ${}^7\text{F}_1$  level amounts to about  $465\text{ cm}^{-1}$ .

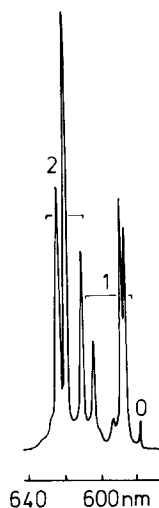


FIG. 3. Emission spectrum of  $\text{La}_{0.99}\text{Eu}_{0.01}\text{BGeO}_5$  (crystalline) at 300 K under CT excitation.

This is a very large splitting. In the Gd compound it is only  $155\text{ cm}^{-1}$ . For  $\text{LaMgB}_5\text{O}_{10}:\text{Eu}$  about  $400\text{ cm}^{-1}$  has been reported, which the authors considered to be a very large splitting (10). In passing we note that the emission spectra of  $\text{LaBGeO}_5:\text{Eu}^{3+}$  and  $\text{LaMgB}_5\text{O}_{10}:\text{Eu}^{3+}$  show some similarity. Also in  $\text{LaMgB}_5\text{O}_{10}$  the site symmetry of La is  $C_1$ , but  $C_{2v}$  was found to be adequate to describe the experimental energy level scheme (10). Such a large  ${}^7F_1$  splitting shows a strong crystal field of electrostatic nature (10).

On the basis of vibrational spectroscopy  $\text{GdBGeO}_5$  and  $\text{LaBGeO}_5$  were assumed to have related structures (1). However, this should be restricted to the presence of ordered  $\text{BO}_4$  and  $\text{GeO}_4$  tetrahedra. The  $\text{Eu}^{3+}$  emission spectra show that the effective lanthanide site symmetry is strongly different.

The excitation spectrum of the  $\text{Eu}^{3+}$  emission of  $\text{LaBGeO}_5:\text{Eu}$  consists of the lines and the CT band of the  $\text{Eu}^{3+}$  ion. The quantum efficiency for line excitation is high. However, for CT excitation the quantum efficiency is much lower, viz. about 20%.

### 3.3. Undoped $\text{GdBGeO}_5$ (Crystalline)

At 4.2 K undoped crystalline  $\text{GdBGeO}_5$  shows a complicated luminescence behavior. The emission spectrum for 275 nm excitation shows equal amounts of  $\text{Gd}^{3+}$  emission (312.5 nm) and a broad-band blue emission with a maximum at 420 nm. For 250 nm excitation the band emission has become dominant (see Fig. 4). This blue band shows an excitation band with a maximum at 255 nm, which corresponds to a weak absorption band with the same position in the diffuse reflection spectrum. The host lattice absorption is at much higher energy.

The excitation spectrum of the  $\text{Gd}^{3+}$  emission shows the  $\text{Gd}^{3+}$  excitation lines ( ${}^8S \rightarrow {}^6I$  and  ${}^6D$ ) and the broad band mentioned above. At room temperature the band emission is practically quenched. Undoped  $\text{LaBGeO}_5$  shows the same broad-band emission, but at longer wavelength; the emission maximum is at about 460 nm. The corresponding excitation band is broad and slightly structured. The maximum is around 280 nm. Also this difference in the broad-band luminescence shows that the crystal structures of  $\text{LaBGeO}_5$  and  $\text{GdBGeO}_5$  are not strongly related.

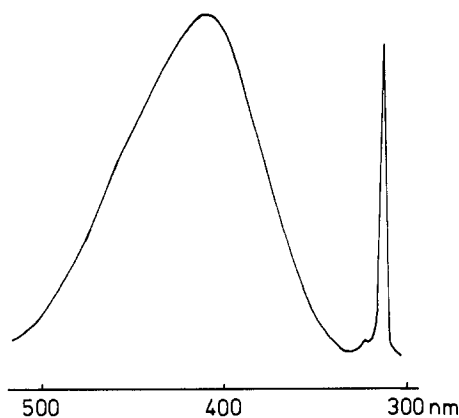


FIG. 4. Emission spectrum of undoped  $\text{GdBGeO}_5$  (crystalline) under 250-nm excitation at 4.2 K.

The interpretation of the spectra is in our opinion as follows: at 4.2 K energy migration over the  $Gd^{3+}$  sublattice is hampered. Excitation into  $Gd^{3+}$  (275 nm) results in  $Gd^{3+}$  trap emission (312.5 nm, see above). However, 275-nm excitation is also absorbed by the tail of the blue-band excitation band, so that some blue emission is excited too. Excitation with 250-nm radiation is absorbed in the band maximum and the blue emission dominates. The weak  $Gd^{3+}$  lines around 250 nm ( $^8S-^6D$ ) cannot compete successfully with the broad band for the excitation radiation. The blue emission is so broad that its short wavelength tail is monitored when the  $Gd^{3+}$  excitation spectrum is measured. Therefore this spectrum contains the broad excitation band. However, the spectra do not show any evidence for energy transfer between the  $Gd^{3+}$  ions and the blue-emitting center.

There is also no reason why this transfer should occur. The spectral overlaps involved are zero ( $Gd^{3+} \rightarrow$  blue center) or very small (blue center  $\rightarrow Gd^{3+}$ ). In addition, comparison of the reflection spectra of undoped  $GdBGeO_5$  and  $Gd_{0.99}Eu_{0.01}BGeO_5$  in the range around 250 nm shows that the concentration of the blue-emitting center must be considerably smaller than the  $Eu^{3+}$  concentration.

This interpretation is confirmed by the 300 K spectra. For 275-nm excitation,  $Gd^{3+}$  emission is observed with the same intensity as at 4.2 K. As shown above the  $Gd^{3+}$  excitation energy migrates over the lattice, but the blue centers are not reached. This follows from the fact that the  $Gd^{3+}$  emission intensity is temperature independent. At 300 K the blue centers will act as quenching centers, since their luminescence is quenched. The  $Gd^{3+}$  emission at 300 K is intrinsic emission (9). It is actually observed at 0.5-nm-shorter wavelength than the  $Gd^{3+}$  trap emission, which yields a trap depth of about  $50\text{ cm}^{-1}$ .

We are left with the problem of the nature

of the blue emitting center. Compounds of  $d^{10}$  ions are known to luminesce (11). This luminescence is not characteristic of the  $d^{10}$  ions involved, but is due to the presence of defects (12). Usually excitation is into the host lattice. In  $GdBGeO_5$  and  $LaBGeO_5$  it is possible to excite into the center itself, so that its concentration must be relatively high. A slight disorder of B and Ge might be a good possibility to explain this center.

### 3.4. X-Ray Excitation

In view of successful research on  $Gd^{3+}$  emission by X-ray excitation (13–15), we investigated also some crystalline samples under X-ray excitation. The results for the borogermanates are disappointing, however. Undoped crystalline  $GdBGeO_5$  under X-ray excitation at 300 K shows mainly broad-band emission. Next to the blue broad band mentioned above, there is another one with a maximum at 350 nm. Further there is  $Tb^{3+}$  and  $Eu^{3+}$  emission (impurities in the 99.999% starting  $Gd_2O_3$ ) and some  $Gd^{3+}$  emission. From this we conclude that the X-ray excitation is mainly trapped by defects and impurities, and not by  $Gd^{3+}$ . In crystalline  $LaBGeO_5:Gd$  there is mainly  $Gd^{3+}$  emission. However, this emission is coupled with  $BO_3^-$  vibrations. Therefore, the X-ray-excited luminescence of  $LaBGeO_5:Gd$  must be very weak and the emission of a second phase, probably  $LaBO_3:Gd$  which emits efficiently, is observed. The weak emission is ascribed to capture of charge carriers by the defect centers. Similar results were obtained for crystalline  $YBGeO_5:Gd$ .

### 3.5. $Gd_{0.99}Bi_{0.01}BGeO_5$ (Crystalline)

As an example of another efficient luminescent center in crystalline  $GdBGeO_5$  we mention  $Bi^{3+}$ . Its luminescence is reasonably well understood (7, 8). The  $Bi^{3+}$  emission shows a broad band with a maximum

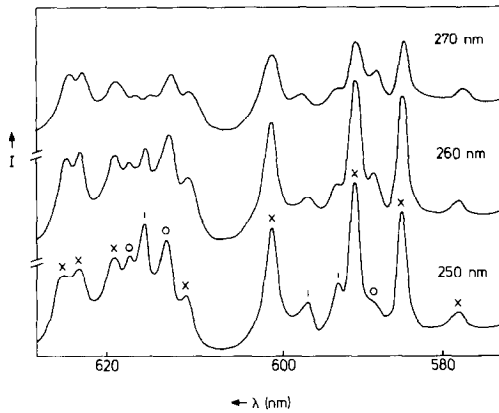


FIG. 5. Emission spectrum of  $CaBPO_5:Eu^{3+}$  (crystalline) in the  ${}^5D_0-{}^7F_{0,1,2}$  region, for different excitation wavelengths in the CT transition.  $T = 4.2$  K.

at 400 nm. The corresponding excitation maximum is at 250 nm, so that the Stokes shift is large, nearly 2 eV. This points to  $Bi^{3+}$  in an asymmetric coordination in the ground state (7). In this composition we observed also  $Gd^{3+}$  emission. We were able to detect two vibronic lines at about 1130 and  $800\text{ cm}^{-1}$  lower energy than the electronic  $Gd^{3+}$  emission line. These values correspond very well with the infrared frequencies given in Ref. (1) for  $BO_4$  and  $GeO_4$  stretching frequencies ( $1120$  and  $804\text{ cm}^{-1}$ , respectively). These vibronic lines were not observed in the X-ray-excited emission spectra which confirms the interpretation given above (section 3.4).

### 3.6. $Ca_{0.995}Eu_{0.005}BPO_5$ and $Ca_{0.99}Na_{0.005}Eu_{0.005}BPO_5$ (Crystalline)

In crystalline  $CaBPO_5$  the  $Eu^{3+}$  ion shows a luminescence of medium efficiency under short-wavelength ultraviolet excitation. The emission spectrum of  $Eu^{3+}$  in  $CaBPO_5$  is rather complex and depends strongly on temperature and excitation wavelength. Figure 5 shows the emission spectrum of the  $Eu^{3+}$  ion in the  ${}^5D_0-{}^7F_{0,1,2}$

region at 4.2 K for different excitation wavelengths in the longer wavelength region of the CT band. From the behavior of the several emission lines for different excitation wavelengths, it follows that at least three kinds of  $Eu^{3+}$  ions are present. The  $Eu^{3+}$  site which is marked by vertical lines in Figs. 5 and 6 can be ascribed to  $Eu^{3+}$  in a second phase. This is concluded from a comparison of this  $Eu^{3+}$  emission to that of  $Ca_2P_2O_7:Eu^{3+}$ . This phosphor was prepared, since  $Ca_2P_2O_7$  was found in the X-ray spectra of our  $CaBPO_5$  samples.

The dominant emission of  $Eu^{3+}$  in  $CaBPO_5$  which has relatively intense  ${}^5D_0-{}^7F_1$  lines corresponds most probably to a  $Eu^{3+}$  ion which replaces the  $Ca^{2+}$  ion in the lattice. This dominant emission consists of one  ${}^5D_0-{}^7F_0$ , three  ${}^5D_0-{}^7F_1$ , and four  ${}^5D_0-{}^7F_2$  lines (Fig. 5, marked by crosses). Like in  $LaBGeO_5:Eu^{3+}$  this points to a symmetry which is higher than  $C_1$ . Another similarity to  $Eu^{3+}$  in  $LaBGeO_5$  is the considerable splitting of the  ${}^5D_0-{}^7F_1$  transition, viz.  $440\text{ cm}^{-1}$  ( $465\text{ cm}^{-1}$  for  $LaBGeO_5$ ). These observations indicate a strong similarity between the hexagonal stillwellite phases of  $CaBPO_5$  and  $LaBGeO_5$ .

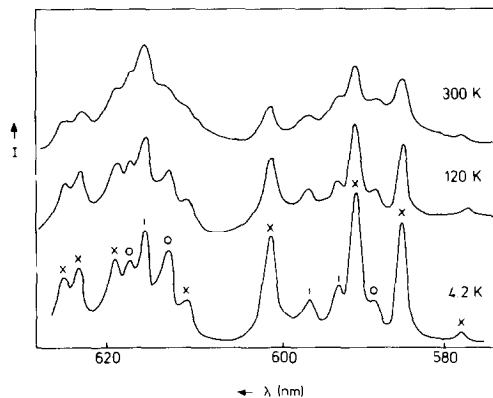


FIG. 6. Temperature dependence of the  $Eu^{3+}$  emission in  $CaBPO_5:Eu^{3+}$  (crystalline) in the  ${}^5D_0-{}^7F_{0,1,2}$  region.  $\lambda_{exc} = 270\text{ nm}$ .

The dominant  $\text{Eu}^{3+}$  emission shows a moderate temperature quenching under CT excitation (Fig. 6). This is ascribed to a thermally activated radiationless relaxation in the CT state. The  $\text{Eu}^{3+}$  ions in a calcium compound have an effective charge and exert an extra attraction on the anions. In the CT state this attraction is weakened (6). The corresponding expansion in the excited state favors temperature-dependent nonradiative relaxation losses.

The emission of  $\text{Eu}^{3+}$  which is marked by circles in Figs. 5 and 6 shows a very different spectral distribution. It is likely that this  $\text{Eu}^{3+}$  site has a calcium vacancy nearby which distorts the site symmetry of  $\text{Eu}^{3+}$  on a  $\text{Ca}^{2+}$  site in  $\text{CaBPO}_5$ . In earlier work (6) we have shown that such a site undergoes a considerable expansion in the excited state, since the surroundings are not able to counteract the expansion in the excited state. This leads to a very strong nonradiative relaxation of excitation energy. The same observation is made for this  $\text{Eu}^{3+}$  site. From Fig. 6 it follows that this emission (o) is almost completely quenched at room temperature.

In  $\text{CaSO}_4:\text{Eu}^{3+}$  (6) we have shown a strong influence of the charge compensator on the luminescence spectra and the quantum efficiency of the  $\text{Eu}^{3+}$  ion. This was explained by the association of  $\text{Eu}^{3+}$  with  $\text{Na}^+$  (shortest cation-cation distance, 3.5 Å). In  $\text{CaBPO}_5:\text{Eu}^{3+}$  this influence could not be observed. In  $\text{CaBPO}_5$  the shortest cation-cation distance amounts also to 3.5 Å (3). Therefore it is likely that sodium does not enter the lattice but reacts rapidly with boric acid to form a melt (16).

The excitation spectrum of the  $\text{Eu}^{3+}$  emission is dominated by the CT band with a maximum at 240 nm. The total quantum efficiency of the  $\text{Eu}^{3+}$  emission upon CT excitation as derived from the excitation spectrum (4) amounts to about 50% at 4.2 K, and decreases to about 30% at 300 K.

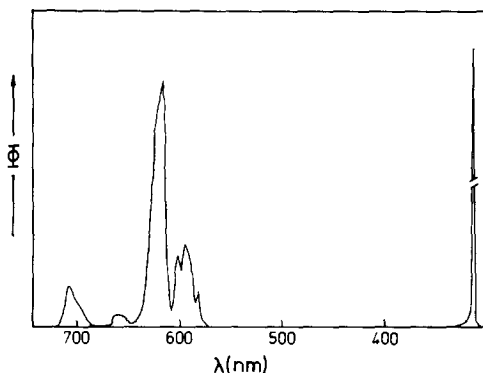


FIG. 7. Emission spectrum of  $\text{GdBGeO}_5:\text{Eu}$  (glass) at 4.2 K.  $\lambda_{\text{exc}} = 275$  nm.

### 3.7. $\text{GdBGeO}_5:\text{Eu}^{3+}$ (Glass)

In the glass modification of  $\text{GdBGeO}_5$  the  $\text{Eu}^{3+}$  ion shows a weak red emission upon CT excitation. Figure 7 shows the emission spectrum at 4.2 K for 275-nm excitation and Fig. 8 the excitation spectrum of the  $\text{Eu}^{3+}$  emission at 300 K. In contrast to that of the crystalline modification, the emission spectrum of the glass consists not only of a  $\text{Gd}^{3+}$  emission line at 313.5 nm, but also of the  $^5\text{D}_0\text{-}^7\text{F}_j$  lines of  $\text{Eu}^{3+}$ . The  $\text{Gd}^{3+}$  emission intensity amounts to about 30% of the total emission intensity. This  $^6\text{P}_{7/2}\text{-}^8\text{S}$  emission of

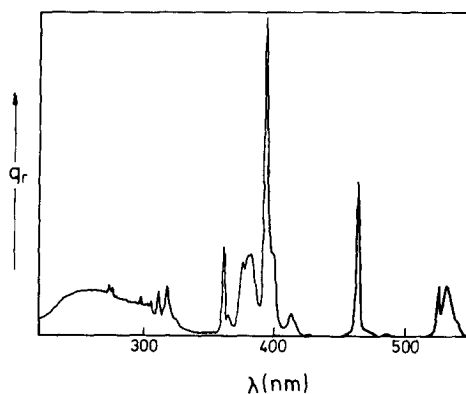


FIG. 8. Excitation spectrum of  $\text{Eu}^{3+}$  in  $\text{GdBGeO}_5:\text{Eu}$  (glass) at 300 K.

$Gd^{3+}$  decreases with temperature to less than 1% of the total emission intensity at 300 K. Since the 275-nm excitation is in both the CT region of the  $Eu^{3+}$  ion and in the  $^8S-^6I$  excitation region of the  $Gd^{3+}$  ion, this means that efficient migration from the  $Gd^{3+}$  ion to the  $Eu^{3+}$  ion takes place. For 250-nm excitation no  $Gd^{3+}$  emission is observed at room temperature and below. The excitation process is the same as that described above for crystalline  $GdBGeO_5:Eu^{3+}$ .

The different relative intensities of the  $Gd^{3+}$  and  $Eu^{3+}$  emissions in the glass and the crystalline modifications upon 275-nm excitation can be understood by a comparison between the  $Eu^{3+}$  CT absorption bands in the crystal and the glass. The difference is striking, since the CT band of  $Eu^{3+}$  in the glass is not only much broader than in the crystal, but it is also much weaker. In the crystal, the  $^8S-^6I$  excitation transition of  $Gd^{3+}$  coincides with the tail of the CT band of  $Eu^{3+}$ , while in the glass the CT band is much broader. The tail of the CT band is at  $\sim 345$  nm and the maximum at 255 nm. Therefore a large part of the excitation energy is, in the case of the glass, directly absorbed by the  $Eu^{3+}$  ions.

The  $Eu^{3+}$  emission pattern does not show clear individual Stark levels for any of the  $^5D_0-^7F_J$  transitions due to the large inhomogeneous broadening. In the crystal the quantum efficiency upon CT excitation amounts to 80% or higher, while in the glass it amounts to 10% or less. This difference in quantum efficiency upon CT excitation between glass and crystal has been observed before (4, 5). We consider it to be a general rule.

### 3.8. $LaBGeO_5:Eu^{3+}$ (Glass)

The  $Eu^{3+}$  ion in the glass modification of  $LaBGeO_5$  shows a weak red emission upon CT excitation. The quantum efficiency upon CT excitation is less than 10%. The difference between the quantum efficiencies of the  $GdBGeO_5:Eu$  and  $LaBGeO_5$  glasses is

smaller than the efficiency difference between glasses and crystals, and/or the efficiency difference between the  $GdBGeO_5:Eu$  and  $LaBGeO_5:Eu$  crystals. The maximum of the CT band is at 265 nm and the onset is at 345 nm.

In contradistinction to the crystalline modifications of  $LaBGeO_5:Eu$  and  $GdBGeO_5:Eu$ , the emission patterns of  $Eu^{3+}$  in the glasses are indistinguishable. This suggests that the site symmetry of the  $Eu^{3+}$  ion in the glasses is similar.

### 3.9. $YBGeO_5:Eu^{3+}$ (Glass)

The glass modification of  $YBGeO_5:Eu$  shows a red emission of weak intensity upon CT excitation. A comparison of the emission spectra of  $Eu^{3+}$  in  $LaBGeO_5$ ,  $GdBGeO_5$ , and  $YBGeO_5$  glass does not present differences of any significance. A comparison of the  $Eu^{3+}$  excitation spectra of these glasses shows no differences for the  $4f^6$  excitation lines, but for the CT band there is a difference in intensity. The intensity of the CT band increases slightly, but significantly, in the sequence La, Gd, Y.

### 3.10. Undoped $GdBGeO_5$ and $LaBGeO_5$ (Glass)

At 4.2 K the luminescence behavior of the glass modification of undoped  $GdBGeO_5$  is less complicated than that of the crystalline modification. The emission spectrum for 275-nm excitation shows only  $Gd^{3+}$  emission. The excitation spectrum of the  $Gd^{3+}$  emission at 4.2 K shows the  $Gd^{3+}$  excitation lines ( $^8S \rightarrow ^6I$  and  $^6D$ ). Figure 9 shows the vibronic sideband of the  $^6P_{7/2}-^8S_{7/2}$  emission transition. Relative to the zero-phonon line the vibronic lines are at  $350\text{ cm}^{-1}$  (Gd-O vibrations),  $800\text{ cm}^{-1}$  (stretching vibration of the  $GeO_4$  tetrahedron (I)), and  $\sim 1340\text{ cm}^{-1}$ . This last peak is most probably due to the stretching vibrations of the  $BO_3$  triangle, and not to vibrations of  $BO_4$  tetrahedra (I). The glass structure (with  $BO_3$  groups) is



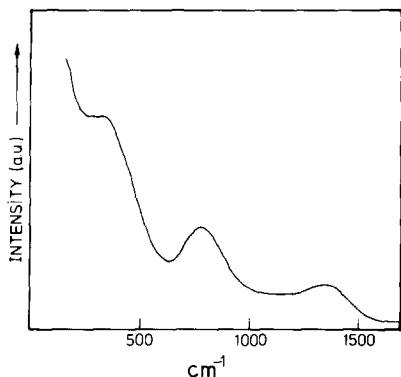


FIG. 9. Vibronic side band of the  $Gd^{3+} {}^6P_{7/2} \rightarrow {}^8S_{7/2}$  emission transition in  $GdBGeO_5$  at 4.2 K. Excitation wavelength is 278 nm.

therefore different from the crystalline structure (with  $BO_4$  groups).

The integrated side band emission intensity amounts to about 5% of the total  $Gd^{3+}$  emission intensity, which is a high value for a glass. The corresponding values for  $LaB_3O_6$  and lithium lanthan phosphate glasses are 1.5 and 2%, respectively (17, 18). The intensity of the vibronic side band seems to be related to the energy of the host lattice absorption band. The lower this energy, the more intense the vibronics (19). For the borogermanate glasses the host lattice absorption is situated at  $\sim 40,000 \text{ cm}^{-1}$ , while for the  $LaB_3O_6$  and lithium lanthan phosphate glasses the host lattice absorption is situated at  $\sim 50,000 \text{ cm}^{-1}$ .

In addition to the  $Gd^{3+}$  luminescence, there is also a broad emission band with a maximum at  $\sim 420 \text{ nm}$  and a shoulder at 480 nm. The excitation band of this luminescence has its maximum at 250 nm. This luminescence is very weak: at 4.2 K its intensity is one order of magnitude weaker than the  $Gd^{3+}$  luminescence. The bands in the glass are broader than in the crystal, so that the spectral overlap  $Gd^{3+} \rightarrow$  blue-emitting center is considerable. This spectral overlap and the energy migration over the  $Gd^{3+}$  ions result in a strong quenching of the  $Gd^{3+}$

luminescence with temperature (see also section 3.3). At room temperature the  $Gd^{3+}$  emission intensity is  $\sim 2\%$  of the emission intensity at 4.2 K. The blue emission intensity does not increase with the same amount as the  $Gd^{3+}$  emission intensity decreases. These blue centers relax nonradiatively and act therefore as quenching centers for the migrating  $Gd^{3+}$  excitation energy. Undoped  $LaBGeO_5$  glass shows a similar broad-band luminescence.

The nature of this luminescence may be of the same type as in the crystalline modifications. Van Die *et al.* (20) have reported similar phenomena for glasses containing even more germanium. In these materials the absorption and emission transitions have shifted to longer wavelengths.

### 3.11. $CaBPO_5:Eu$ (Glass)

Europium in the glass modification of  $CaBPO_5$  shows an intense white emission upon UV excitation as a result of a combination of broad-band emission from  $Eu^{2+}$  (blue-green) and red  ${}^5D_0 \rightarrow {}^7F_J$  line emission of  $Eu^{3+}$ .

The  $Eu^{3+}$  emission spectrum is similar to the emission spectra of  $Eu^{3+}$  in the other glasses. The excitation spectrum, however, shows a large difference. The quantum efficiency upon CT excitation is very low ( $q < 5\%$ ). This is not too surprising in view of the fact that this efficiency is already low in the crystalline modification. However, there is a second reason: a certain amount of the light emitted by the excitation source is absorbed by  $Eu^{2+}$  and subsequently does not reach the  $Eu^{3+}$  ions.

Upon excitation into the  $4f^65d$  band, the  $Eu^{2+}$  ion shows a blue-green emission of medium intensity. The maximum of the emission band varies with excitation wavelength, for example, it is situated at 440 nm upon 390-nm excitation, and at 420 nm upon 260-nm excitation. The maximum of the broad  $Eu^{2+}$  excitation band is situated at  $\sim 370 \text{ nm}$ . The Stokes shift is  $(3750 \pm 500)$

TABLE I

THE LUMINESCENCE EFFICIENCY OF THE  $\text{Eu}^{3+}$  ION IN DIFFERENT HOST MATERIALS UPON CT EXCITATION AT ROOM TEMPERATURE

Gd $\text{BGeO}_5$	(crystalline)	$\geq 80\%$
Ca $\text{BPO}_5$	(crystalline)	30%
La $\text{BGeO}_5$	(crystalline)	20%
Y $\text{BGeO}_5$	(glass)	$\leq 20\%$
Gd $\text{BGeO}_5$	(glass)	$\leq 10\%$
La $\text{BGeO}_5$	(glass)	$< 10\%$
Ca $\text{BPO}_5$	(glass)	$< 5\%$

$\text{cm}^{-1}$ . This indicates a certain inhomogeneous broadening. This is also shown by the fact that at 4.2 K a small amount ( $\sim 0.5\%$ ) of the emission is  $4f^7 (^6\text{P}_{7/2}) \rightarrow 4f^7 (^8\text{S}_{7/2})$  line emission at 360 nm. This implies that for some of the  $\text{Eu}^{2+}$  ions the  $^6\text{P}_{7/2}$  level is situated at a lower energy than the lowest  $4f^6 5d$  level.

There is a striking analogy between the emission of  $\text{Eu}^{2+}$  in this glass and that of  $\text{Cr}^{3+}$  in (especially) borate glass (21). In both cases a small amount of line emission has been observed in addition to a broad band emission. However, whereas for  $\text{Cr}^{3+}$  the high field  $\text{Cr}^{3+}$  ions give the line emission (21), for  $\text{Eu}^{2+}$  the low field  $\text{Eu}^{2+}$  ions give the line emission (22).

The quantum efficiency of the  $\text{Eu}^{2+}$  luminescence is strongly temperature dependent. The emission intensity at room temperature is  $\sim 35\%$  of the emission intensity at 4.2 K. Elsewhere we have shown that  $d \rightarrow f$  emission of rare earth ions in glasses may be very efficient if the excitation energy is in the short wavelength UV region (say  $\lambda < 300$  nm) (5, 17). The low  $\text{Eu}^{2+}$  efficiency at 300 K is, therefore, ascribed in the first place to the low position of the emitting  $4f^6 5d$  level.

#### 4. General Discussion of the $\text{Eu}^{3+}$ Quantum Efficiency upon CT Excitation

Table I shows the estimated quantum efficiencies of the  $\text{Eu}^{3+}$  luminescence in both

the crystalline and glass modifications of the borogermanates and the borophosphates upon CT excitation.

We note the following trends:

(a) For crystals the efficiency depends on the size and the charge of the host lattice ion for which  $\text{Eu}^{3+}$  ion is substituted. In Gd $\text{BGeO}_5:\text{Eu}$  the efficiency is high. The  $\text{Eu}^{3+}$  ion does not expand much in the excited state. As a result the difference between the equilibrium distances of the excited state and the ground state is small: the CT state feeds the higher  $4f^6$  levels efficiently. This is also the case in Gd $_2\text{O}_3:\text{Eu}^{3+}$  and other phosphors in which  $\text{Eu}^{3+}$  replaces  $\text{Gd}^{3+}$  (23).

In Ca $\text{BPO}_5:\text{Eu}$  and La $\text{BGeO}_5:\text{Eu}$  the efficiency is much lower. The luminescence efficiency of  $\text{Eu}^{3+}$  on a  $\text{Ca}^{2+}$  site tends to be low for CT excitation (6). The  $\text{Eu}^{3+}$  ion has an effective positive charge on these sites, which enables it to expand strongly upon excitation. This results in a large equilibrium distance and a low efficiency (6).

The  $\text{Eu}^{3+}$  ion replacing a trivalent ion which has a larger ionic radius ( $\text{La}^{3+}$ ) can also be considered to bear an effective positive charge (24). Therefore the efficiency of the  $\text{Eu}^{3+}$  luminescence in lanthanum compounds is usually low (23).

(b) The efficiency of the  $\text{Eu}^{3+}$  luminescence upon CT excitation in glasses is much lower than in the crystalline modification. This has been observed and interpreted before (4, 5). The glass structure is considered to be less stiff than the crystalline structure so that expansion after excitation is not strongly restricted by the surroundings of the luminescent ions. This makes nonradiative relaxation to the ground state possible.

In order to confirm this model further we measured the density of a number of samples. The density of crystalline Gd $\text{BGeO}_5$  appears to be  $5.82 \text{ g cm}^{-3}$  and the density of the glass modification of Gd $\text{BGeO}_5$   $5.66 \text{ g cm}^{-3}$ , so that the glass modification is  $\sim 3\%$

less dense than the crystalline modification. This implies that the interatomic distances in the glass are 1% to a few percent longer depending on whether the density difference is ascribed to the total glass composition or to the surroundings of the network modifier. For the Eu–O distance ( $\sim 2.4 \text{ \AA}$ ) this means a roughly  $0.05 \text{ \AA}$  longer distance in the glass than in the crystal. If this equals also the increase of  $\Delta Q$ , the difference between the equilibrium distances in excited state and ground state, this is most probably responsible for the dominance of the nonradiative transition in the glass modifications (25, 26).

(c) For the glasses the efficiency decreases in the sequence Y, Gd, La, Ca. This difference in efficiency shows that in a glass not only the network-forming ions influence the luminescent properties of the dopant ion, but also the network-modifier ions.

This influence is well known in the case of crystalline compositions, but to our knowledge this influence of network modifiers in glasses on the luminescence efficiency has not been observed before. This is most probably due to the fact that luminescence studies on glasses with high amounts of highly charged modifier ions are scarce.

Our results however show some analogy with a recent study by Shelby and Kohli on the influence of the ionic radius of the modifier ions on the expansion coefficient of glasses (27). They observed that the expansion coefficient is directly proportional to the ionic size of the modifier ion. It is not hard to imagine that there is a relation between overall expansion upon thermal heating of a solid and local expansion upon excitation of an ion in that solid.

## Conclusion

From the present study we conclude that the quantum efficiency of the luminescence of the  $\text{Eu}^{3+}$  ion upon charge-transfer excitation is influenced by

(a) the density of the host material. The crystalline modification of  $\text{GdBGdO}_5:\text{Eu}$  shows a very efficient luminescence upon CT excitation, while the efficiency of the glass modification of this material is low. This runs parallel with the earlier observations that the efficiency in the glass modification is always much lower in the corresponding crystalline modification. This low quantum efficiency of the  $\text{Eu}^{3+}$  emission upon CT excitation is due to nonradiative transitions from the CT state to the ground state due to a large parabolae offset.

(b) the size of the network modifier ion. For the  $\text{LnBGdO}_5:\text{Eu}$  glasses the efficiency increases in the sequence  $\text{Ln} = \text{La, Gd, Y}$ .

The Europium-doped  $\text{CaBPO}_5$  glass shows next to the  $4f^65d \rightarrow 4f^7(^8\text{S}_{7/2})$  broad band emission the  $4f^7(^6\text{P}_{7/2}) \rightarrow 4f^7(^8\text{S}_{7/2})$  line emission of divalent europium. It is the first time this has been observed from a glass.

## References

1. A. RULMONT AND P. TARTE, *J. Solid State Chem.* **75**, 244 (1988).
2. G. V. LYSANOVA, B. F. DZHURINSKII, M. G. KOMOVA, V. I. TSARYUK, AND I. V. TANANAEV, *Izv. Akad. Nauk SSSR, Neorg. Mater.* **25**, 632 (1989).
3. A. A. VORONKOV AND YU. A. PYATENKO, *Sov. Phys. Crystallogr.* **12**, 214 (1967).
4. J. W. M. VERWEY, G. J. DIRKSEN, AND G. BLASSE, *J. Non-Cryst. Solids* **107**, 49 (1988).
5. J. W. M. VERWEY AND G. BLASSE, *Mater. Chem. Phys.* **25**, 91 (1990).
6. D. VAN DER VOORT AND G. BLASSE, *J. Solid State Chem.*, **87**, 350 (1990).
7. G. BLASSE, *Prog. Solid State Chem.* **18**, 79 (1988).
8. G. BLASSE, *Chem. Mater.* **1**, 294 (1989).
9. A. J. DE VRIES, M. F. HAZENKAMP, AND G. BLASSE, *J. Lumin.* **42**, 275 (1988).
10. J. HÖLSÄ AND M. LESKALÄ, *Mol. Phys.* **54**, 657 (1985).
11. G. BLASSE AND A. BRIL, *Mater. Res. Bull.* **5**, 231 (1970).
12. T. HARWIG AND F. KELLENBONK, *J. Solid State Chem.* **24**, 255 (1978).
13. G. BLASSE AND L. H. BRIXNER, *Eur. J. Solid State Inorg. Chem.* **26**, 367 (1989).
14. G. BLASSE, L. H. BRIXNER, AND S. MROCKOWSKI, *J. Solid State Chem.* **82**, 303 (1989).

15. L. H. BRIXNER AND G. BLASSE, *J. Electrochem. Soc.* **136**, 3529 (1989).
16. D. VAN DER VOORT, R. VAN DOORN, AND G. BLASSE, to be published.
17. J. W. M. VERWEY, G. F. IMBUSCH, AND G. BLASSE, *J. Phys. Chem. Solids* **50**, 813 (1989).
18. J. W. M. VERWEY AND G. BLASSE, *Chem. Mater.* **2**, 458 (1990).
19. J. DEXPERT-GHYS AND F. AUZEL, *J. Chem. Phys.* **80**, 4003 (1984).
20. A. VAN DIE, A. C. H. I. LEENAERS, G. BLASSE, AND W. F. VAN DER WEG, *J. Non-Cryst. Solids* **99**, 32 (1988).
21. A. VAN DIE, G. BLASSE, AND W. F. VAN DER WEG, *Mater. Chem. Phys.* **14**, 513 (1986).
22. A. MEYERINK AND G. BLASSE, *J. Lumin.* **43**, 283 (1989).
23. G. BLASSE, "Handbook of the Physics and Chemistry of Rare Earths" (K. A. Gschneidner, Jr. and L. Eyring, Eds.), Chap. 34, North-Holland, Amsterdam (1979).
24. R. L. FULLER AND D. S. MCCLURE, *J. Lumin.* **45**, 354 (1990).
25. G. BLASSE, in "Radiationless Processes" (B. DiBartolo, Ed.), p. 287, Plenum, New York (1980).
26. G. BLASSE, in "Advances in Nonradiative Processes in Solids" (B. DiBartolo, Ed.), in press, Plenum, New York (1990).
27. J. E. SHELBY AND J. T. KOHLI, *J. Amer. Ceram. Soc.* **73**, 39 (1990).